THE STRUCTURAL DESIGN OF TALL AND SPECIAL BUILDINGS
Struct. Design Tall Spec. Build. **20**, 928–950 (2011)
Published online 8 March 2010 in Wiley Online Library (wileyonlinelibrary.com/journal/tal). DOI: 10.1002/tal.568

Using Orthogonal Pairs of Rollers on Concave Beds (OPRCB) as a base isolation system—part i: analytical, experimental and numerical studies of OPRCB isolators

Mahmood Hosseini[1]*,† and Amirhossein Soroor[2]

[1] *Structural Engineering Research Center, The International Institute of Earthquake Engineering and Seismology (IIEES), Tehran, Iran [correction made here after initial online publication]*
[2] *Earthquake Engineering Department, School of Engineering, Science and Research Branch of The Islamic Azad University (IAU), Tehran, Iran [correction made here after initial online publication]*

SUMMARY

A somehow new isolating system is introduced for short- to mid-rise buildings. It does not need high technology for manufacturing and is not costly, contrary to other existing systems like lead-rubber bearing or friction pendulum bearing systems. Each isolator of the proposed system consists of two Orthogonal Pairs of Rollers on Concave Beds (OPRCB). Rolling rods installed in two orthogonal directions make possible the movement of the superstructure in all horizontal directions. The concave beds, in addition to giving the system both restoring and re-centring capabilities, make the force–displacement behaviour of the isolators to be of hardening type. The results of the studies on the specifications of the proposed isolating system and its application to buildings can be presented in two parts. Part I relates to the analytical formulations and the results of experimental and numerical studies of the system's mechanical feature, including its dynamical properties, and part II focuses on the effectiveness of the proposed isolation system in seismic response reduction of low- to mid-rise buildings. In part I of the work, presented in this paper, at first general features of the OPRCB isolator are explained and the analytical formulation, governing its dynamic motion, is derived and discussed in detail. Then, the results of experimental and numerical investigations, including the lateral load displacement relationship of the OPRCB isolators under various vertical loads, obtained by both Finite Element Analyses (FEA) and laboratory tests are presented (FEA results have been verified by the laboratory tests). Finally, responses of some Single Degree of Freedom (SDOF) systems, isolated by OPRCB devices, subjected to simultaneous effect of horizontal and vertical ground motions, are presented and compared with responses of their fixed-base counterparts. Based on the numerical calculations, it is observed that the oscillation period of the isolated SDOF system is independent of its mass, the initial amplitude of its free vibration response and the value of rolling resistance coefficient. With regard to seismic response reduction it is seen that the amount of absolute accelerations in the SDOF systems, isolated by OPRCB devices, can be reduced drastically in comparison with the fixed-base systems. Results also show that if the rollers and cylindrical beds are made of high-strength steel materials, the system can be used effectively under the vertical loads of about the axial forces of ground floor columns in ordinary buildings up to 14 storeys. Copyright © 2010 John Wiley & Sons, Ltd.

1. INTRODUCTION

The base isolation technique is based on the simple concept of decoupling the building or structure from the horizontal components of the ground motion. This can be done by interposing structural elements with low horizontal stiffness between the structure and the foundation. Seismic isolation gives the structure a fundamental frequency that is much lower than both the frequency of fixed-based structure and the predominant frequencies of ground motions. The first dynamic mode of the isolated structure involves deformation only in the isolation system, while its higher modes which are orthogo-

* Correspondence to: Mahmood Hosseini, Structural Engineering Research Center, The International Institute of Earthquake Engineering and Seismology (IIEES), No. 21 Arghaven, North Dibaji St., Farmanieh, Tehran 19537, Iran
† E-mail: hosseini@iiees.ac.ir
This article was published online on 8 March 2010. An error was subsequently identified. This notice is included in the online and print versions to indicate that both have been corrected [24 June 2010].

nal to the first mode do not participate so much in the motion, so that the high energy in the ground motion at these higher frequencies cannot be transmitted into the structure (Naeim and Kelly, 1999). Although the base isolation is not a new idea and goes back to more than 100 years ago (Buckle and Mayes, 1990), prior to 1980, almost all lateral force resisting systems in the seismic areas of the world were composed entirely of conventional materials (Hart and Wong, 2000).

Very few cases on the practical use of isolators in buildings before the 1980s have been reported, of which, one relates to the construction of two buildings by using an isolation layer consisting of top and bottom steel plates (plane or curved) with rollers between them in central China between 1968 and 1978 (Zhou, 2001). Zhou has mentioned that the main advantage of this isolation device is that it effectively isolates the ground motion, and the main problem is that the device needs careful maintenance to ensure effective operation over its long working lifetime (Zhou *et al.*, 1988). Kelly (1983) discussed the economic feasibility of rehabilitation by seismic isolation technique, however, the first professional effort within the engineering community for developing the base-isolated buildings design provisions was started by Dr. Ron Mayes in California in the late 80s, that resulted in the first set of design provisions for base-isolated buildings in the 1991 Uniform Building Code (Hart and Wong, 2000).

During recent decades, many seismic isolation devices have been developed to deal with the growing need for practical applications. Among them, lead-rubber bearing (LRB), high-damping rubber bearing (HRB) and friction pendulum system (FPS) are well-developed devices, because these devices meet better the three major criteria of simplicity, reliability and cost-effectiveness. Obviously, extensive experimental and numerical investigations are required to achieve the three aforementioned criteria for any practical isolation device. The FPS adopts a curved sliding surface so that the restoring force can be provided by the weight of its supported structure. However, the curved sliding surface may result in increased horizontal force with larger displacement (Naeim and Kelly, 1999).

Although using rollers as seismic isolators is an old idea, very few academic studies have been performed in this regard prior to 1990; however, several works have been published since the early 90s. The use of free rolling rods under basement, both analytically (Lin and Hone, 1993) and experimentally, by shaking table tests (Lin *et al.*, 1995), has been studied for a one-storey frame. Jangid (1995) has also studied a sliding isolation system in the form of circular rolling rods. In those works, the rolling rods were considered without any restoring force. As a result, there were more peak and residual base displacements. To overcome this difficulty, the use of elliptical rods instead of the circular rods was suggested (Jangid and Londhe, 1998; Londhe and Jangid, 1999). However, the elliptical rolling rods may induce some vertical acceleration into the superstructure. The other alternative was to use some re-centring device along with circular rolling rods to provide the restoring force for controlling the base displacement. In this regard, Jangid (2000) has investigated the seismic response of flexible multi-storey buildings mounted on rolling rods with a re-centring device to non-stationary earthquake excitation. He has shown that the rolling rods are quite effective in reducing the earthquake response of the superstructure and that the presence of a re-centring device significantly reduces the relative base displacement without transmitting additional accelerations into the superstructure.

Another study has been done also on sloping surface roller bearing and its lateral stiffness measurement (Lee and Liang, 2003). A sloped rolling-type bearing (RTB), which utilizes the concept of a steel cylinder rolling on a V-shape surface, has also been proposed (Lee *et al.*, 2003). Their seismic isolation bearing comprises a lower plate, an upper plate and a cylindrical roller in rolling contact with an upwardly facing bearing surface of the lower plate and a downwardly facing surface of the upper plate. The lower plate is fixable to a base, while the upper plate is fixable to a superstructure. One or both bearing surfaces are sloped to form a central trough at which the cylindrical roller resides under normal weight of the superstructure, and toward which the roller is biased when relative displacement between the lower and upper plates occurs to provide a constant restoring force. A pair of sidewall members are fixed to the lower plate to withstand strong forces directed laterally with respect to the isolation axis along which rolling displacement occurs, and a pair of sliding guides, carried one at each end of the roller, provide dry frictional damping as they engage an inner wall surface of a corresponding sidewall member.

RTB isolators have also been used in seismic isolation tests of a bridge model (Tsai *et al.*, 2006; Tsai *et al.*, 2007). Tsai and his colleagues have conducted shaking table tests to investigate the seismic

DOI: 10.1002/tal

behaviour of a 1/7.5 scaled bridge model isolated by the RTBs. Their scaled bridge model has been designed to simulate one vibration unit of a multi-span, simply-supported highway bridge. The RTB is composed of a steel cylinder (roller) and two V-shape steel plates. In that study, a constant horizontal force was transmitted through the RTB when the sloped rolling mechanissm was triggered. Since the rolling resistance is always less than the sliding resistance on the same surface, the horizontal force transmitted by the RTB shall be less than that by a sliding bearing. Also, the restoring force of the RTB may be provided by the parallel component of the gravity load on the roller to the sloped surface. Their test results have verified that the sloped rolling-type bearing is an effective seismic isolation device.

The relatively high costs of using isolating systems as well as high technology required for production and installation of isolators have been two main reasons for the slow development of this technique in developing countries. Hosseini and Kangarloo (2007) introduced a somehow new isolating system that does not need high technology for construction, and is not as costly as other existing systems like lead-rubber bearing or friction pendulum bearing systems. The proposed system consists of two pairs of orthogonal steel rollers, making possible the movement of the superstructure in all horizontal directions. Rollers move on a cylindrical steel bed, which gives a restoring capability to the system. The two rollers of each pair are connected together at both ends with two plates with hinges. This makes the two rollers of each pair to move together and have the same elevation in the cylindrical bed at any instant during the earthquake. The natural period of the system is almost independent of the superstructure mass, and is basically a function of r/R ratio in which r is the radius of the rollers and R is the radius of the cylindrical beds. In that study to obtain the appropriate values of r and R to reach a specific value of the natural period of the isolated system, in addition to analytical hand calculations, some numerical Finite Element calculations have been performed, and verified by laboratory tests.

In recent years, some studies have also been performed with regard to the nonlinear behaviour of rolling isolation systems. Chung and his colleagues (2009) have studied the dynamic behaviour of a nonlinear rolling isolation system. Mentioning that the linear isolator has fixed vibration frequency, and therefore, when structures with these linear isolators are located near a fault, it may cause resonance and large displacement response, they have suggested that nonlinear isolation may avoid this situation. They have studied an eccentric nonlinear rolling isolator with a parameter, which is the eccentricity of the pin connection of the mass block (facility) to the circular isolator. They have stated that if the eccentricity is not equal to zero, the dynamic response is nonlinear rolling behaviour. They have derived an equation of motion of the isolation system and have shown that frequency of the isolator increases with the eccentricity under the same initial angle. They have also scrutinized the influence of the eccentricity to the effect of isolation. Finally, they have verified the feasibility of the proposed isolation device numerically. They have claimed that if their proposed isolator is designed properly, it is effective for far-field earthquake (El Centro earthquake), and even though the linearized frequency of the proposed isolator falls into the dominant frequency range of near-fault earthquake (Chi-Chi earthquake), resonance can be avoided due to nonlinearity.

Lee and his colleagues (2008) have studied a roller seismic isolation bearing for highway bridges, consisting of cylindrical rollers on V-shaped sloping surfaces. The bearing is characterized by a constant spectral acceleration under horizontal ground motions and by a self-centring capability, which are two desirable properties for seismic applications. The former makes resonance less likely to occur between the bearing and horizontal earthquakes while the latter guarantees the bridge superstructure can self-centre to its original position after earthquakes. To provide supplemental energy dissipation to reduce the seismic responses, the bearing is designed with built-in sliding friction mechanisms. The study first presents the acceleration responses of and forces acting on the bearing under base excitation. Next, the governing equation of horizontal motions, the base shear–horizontal displacement relationship, and the conditions for self-centring for the rollers to maintain in contact with the bearing plates and for rolling without sliding are discussed.

Following the studies of Hosseini and Kangarloo (2007), recently, Hosseini and Soroor (2009), calling the proposed system 'Orthogonal Pairs of Rods on Concave Beds (OPRCB)', continued the studies on this type of isolating system. This paper presents the first part of the detailed experimental and numerical investigations, of which the results include the lateral load displacement relationship of the rollers pair under various vertical loads, obtained by both finite element analyses and laboratory

DOI: 10.1002/tal

tests of a prototype sample, which have verified the results of finite element calculations, and the seismic responses of isolated Single Degree of Freedom (SDOF) systems and their fixed-base counterparts, subjected to simultaneous effect of horizontal and vertical ground motions. In the next sections, at first, the general features of the OPRCB isolators are introduced, then the analytical formulation governing the motion of SDOF systems isolated by OPRCB isolators is discussed. After that, the results of the Numerical and Experimental Studies of OPRCB Isolators are presented, followed by the study on efficiency of OPRCB devices in seismic isolation; and finally some concluding remarks are given.

2. GENERAL FEATURES OF THE OPRCB DEVICES

Main parts of the proposed isolator, called Orthogonal Pairs of Rods on Concave Beds (OPRCB), are shown schematically in Figure 1; its prototype sample in Figure 2; the geometrical features of its prototype sample in Figure 3; and the specifications of its manufacturing steel material in Tables 1 and 2.

It can be seen in Figures 1–3 that because of the orthogonal setting of rollers pairs, the top plate can move in all horizontal directions. The concave beds give a restoring capability to the system. The two rollers of each pair are connected together at both ends with two plates with hinge connections as shown in Figure 4, to make the two rollers of each pair move together and have the same elevation in the cylindrical beds at any instant during an earthquake; otherwise they may lose their parallel status and synchronized motion because of seismic disturbances, particularly the vertical excitations of ground motions.

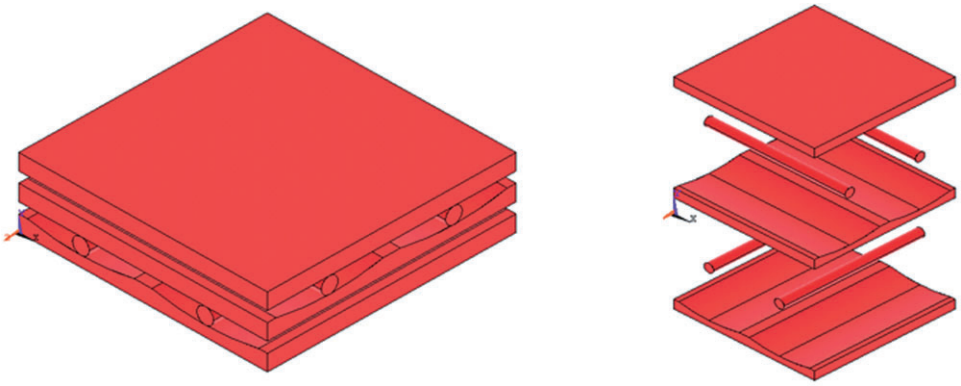

Figure 1. The proposed OPRCB base isolation system.

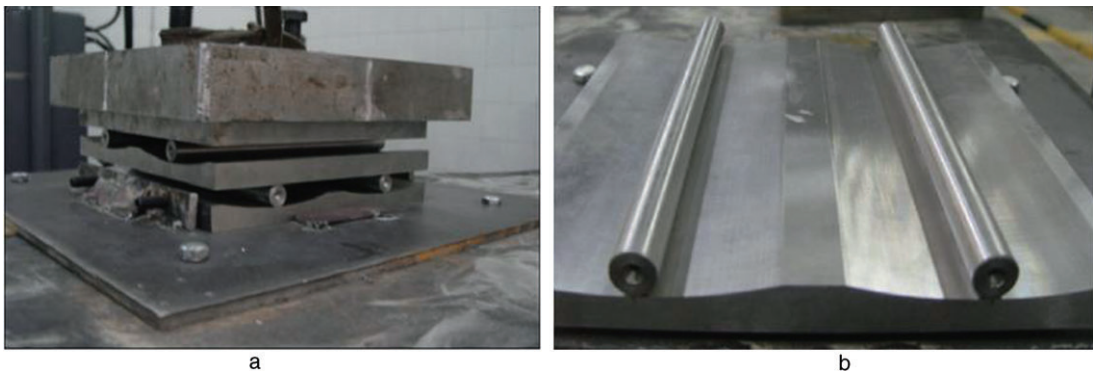

Figure 2. The prototype sample of the OPRCB isolator. (a) The set of the prototype OPRCB. (b) One pair of rolling rods on their concave beds.

DOI: 10.1002/tal

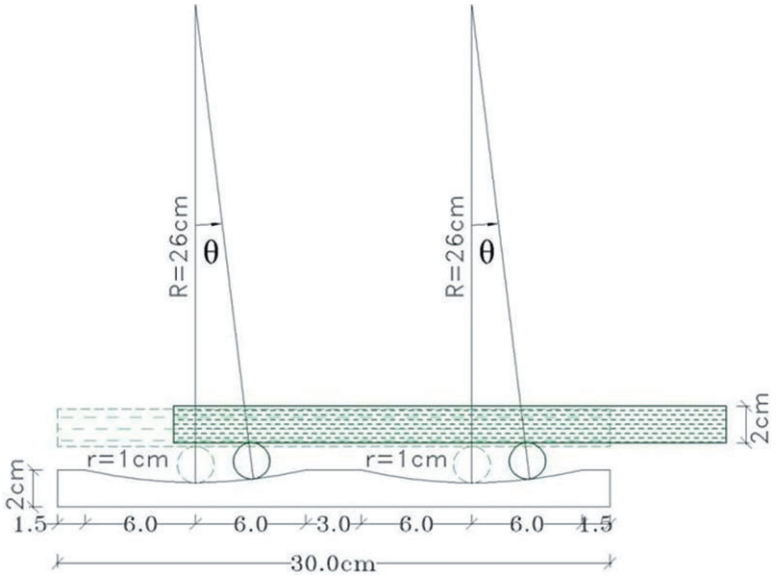

Figure 3. The geometric features of the lower half and the middle plate of the prototype set of OPRCB isolator.

Table 1. Assigned names and usage of the used steel alloy for making the OPRCB parts (Ref: Wegst-Key to steel, 2007).

	Assigned name in different standards							
Steel group	IASC MARK	SYMBOL DIN	DIN	STARSTAHL ROCHLING	B.S	SWEDEN	A.I.S.I SAE/ ASTM	Application
Hot forming and heat treatment (high quality alloyed)	IASC7225	42CrMo4	1.7225	MO40	708M40	42CrMo4	4140(SAE)	For automotive and aircraft components with high toughness as axle journals, gears, tyres, push rods, rollers in concrete and steel industries, high resistance bolts

Table 2. The specifications of the steel material of the OPRCB isolators (Ref: Wegst-Key to steel, 2007)

chemical composition													
C		Cr		Mn		Mo		P		S		Si	
from	to	from	to	from	to	from	to	from	to	from	to	from	to
0.38	0.45	0.8	1.2	0.6	1	0.2	0.3	0	0.02	0	0.015	0	0.6
yielding stress is 900 N/mm^2 based on Wegst-Key to Steel, 2007													

DOI: 10.1002/tal

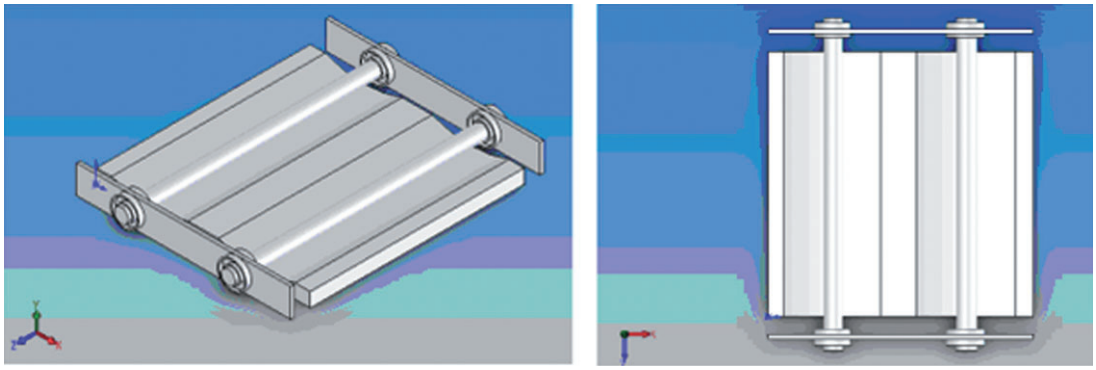

Figure 4. Using end plates with ball-bearing connection for synchronized motion of rollers pair.

$$\sum F_x = 0 \rightarrow R_b \sin\frac{\theta}{2} = F \quad \sum F_y = 0 \rightarrow R_b \cos\frac{\theta}{2} = W$$

$$F = W \tan\frac{\theta}{2}$$

$$F_{f,\text{req}} = R_b \sin\frac{\theta}{2} = F$$

$$N = R_b \cos\frac{\theta}{2} = W$$

$$F_{f,\max} = \mu_s N = \mu_s W$$

$$F_{f,\text{req}} = F = W \tan\frac{\theta}{2} \le \mu_s W$$

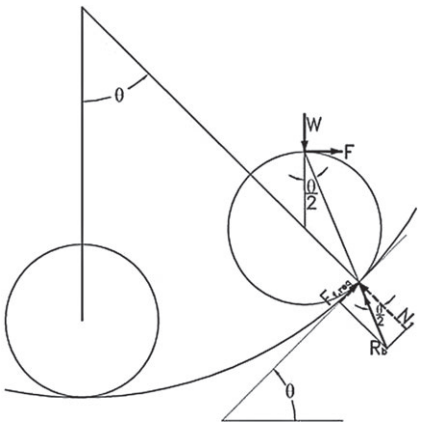

Hence the required condition for rolling without sliding is $\tan\frac{\theta}{2} \le \mu_s = 0{\cdot}35.$

Figure 5. Conditions for rolling of a roller on a sloped or curved surface without sliding.

3. ANALYTICAL STUDY OF THE OPRCB ISOLATORS

The first important point which should be taken into consideration, in the study of a roller on a sloped or curved surface, is the condition governing its sliding and/or rolling motion. Figure 5 illustrates the formulations engaged in the static equilibrium of a cylindrical rod staying on the internal surface of a cylindrical bed, based on which the condition for the rolling of the rod without slippage is derived.

In Figure 5, W is the amount of weight being supported by the roller; R_b is the reaction of cylindrical bed; F is the force tending to roll up the rod; $F_{f,\text{req}}$ is the component of R_b parallel to the slope, which can be looked at as the amount of friction force required for the prevention of the rod from slippage; N is the component of R_b perpendicular to the slope, which, if multiplied by the coefficient of sliding friction, μ_s, gives $F_{f,\max}$ or the maximum existing sliding friction force between the roller and the bed. Now, denoting the amount of weight of a single mass m_b, resting on a set of OPRCB isolator, by $W = m_b\, g$, half of this value will be carried by each roller as shown in Figure 6.

In Figure 6(a), K_b and C_b are stiffness and damping coefficient of the SDOF system, resulting in spring force, F_s, and damping force, F_d, during the system motion, F_{sr} is the amount of sliding friction force required for preventing the rollers from slippage during their motion. F_{r1} is the rolling resistance force between the rollers and their bed, and N_1 is reaction force normal to the contact surfaces between rollers and their bed. In Figure 6(b), F_i is the internal horizontal force between the rollers and the mass above them, and N_2 is the vertical force acting at the top of the rollers during earthquake. The motion

DOI: 10.1002/tal

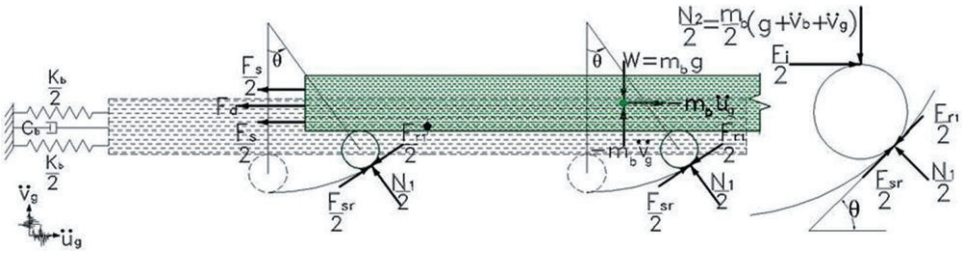

Figure 6. The forces engaged in: (a) the motion of an SDOF system subjected to horizontal and vertical components of ground motion, u_g and v_g; and (b) the equilibrium of rollers, for deriving the Lagrange equation of motion in the presence of rolling resistance.

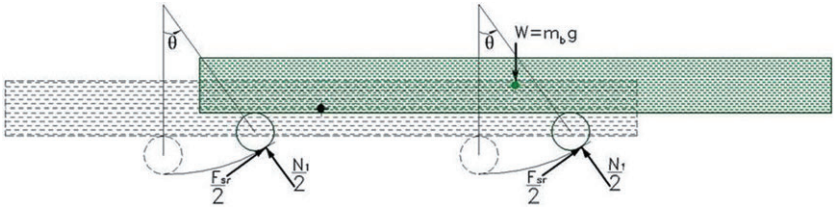

Figure 7. The forces engaged in the free vibration of an SDOF system on OPRCB device for deriving the Lagrange equation of motion in the absence of rolling friction.

of such an SDOF system (considering the motion of only one pair of rollers in one direction) subjected to horizontal and vertical components of earthquake ground motion can be formulated by using Lagrange equation, as discussed hereinafter. Stiffness and damping forces have not been excluded from these formulations to keep the opportunity of comparing the isolated and non-isolated systems. It should be noted that as the mass moves in one direction, the gravity load gets some offset with respect to the centre point of the OPRCB isolator, and this can change the values of load being carried by each of the two rollers. However, this change is not so much remarkable to make the rollers' behaviour significantly different from each other, and therefore, each of the interacting forces between rollers and their bed, and the mass above them, has been assumed to be half of the total value of that force for the two rollers. To derive the equation of motion for this SDOF system, it is necessary to start from the basic case, shown in Figure 7, in which there is no rolling friction and no earthquake excitation, and the only restoring force of the system is the parallel-to-slope component of the gravity force of the system mass (weight of rollers are negligible when compared with the weight of the system mass).

There is a deliberate point in extracting the equation of motion of this system in the difference between the amount of horizontal displacement of the base mass and that of the rollers. In fact, as shown in Figure 8, as each roller moves on its curved bed, its top point, whose movement is exactly the movement of the base mass, has an instantaneous infinitesimal displacement vector $\overrightarrow{ds_b}$ which has two components of du_b and dv_b, respectively in horizontal and vertical directions.

Now, to calculate du_b and dv_b, noting to Figure 8, one can write:

$$(R-r)d\theta = r\,d\theta_r \tag{1}$$

and

$$r_t = 2r\cos\frac{\theta}{2} \tag{2}$$

where r_t is instantaneous radius of rotation of the roller's top point, the length of $\overrightarrow{ds_b}$ can be written as:

$$ds_b = r_t d\theta_r = 2r\cos\frac{\theta}{2}d\theta_r = 2(R-r)\cos\frac{\theta}{2}d\theta \tag{3}$$

DOI: 10.1002/tal

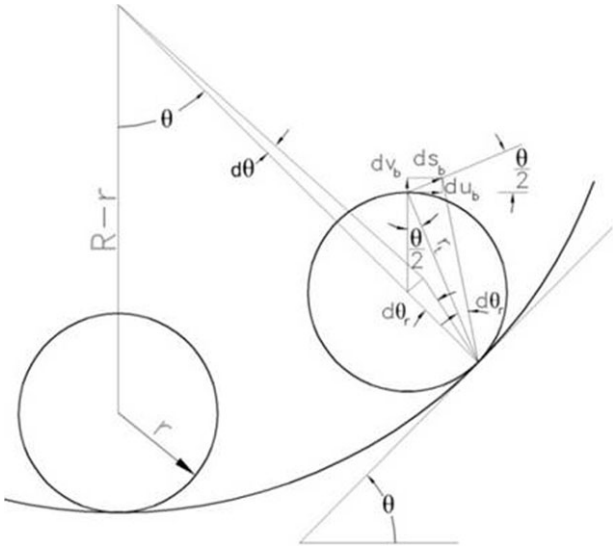

Figure 8. How the infinitesimal movement of the roller affects its top movement.

Hence, du_b and dv_b are:

$$du_b = 2(R-r)\cos^2\frac{\theta}{2}d\theta = (R-r)(1+\cos\theta)d\theta \tag{4}$$

$$dv_b = 2(R-r)\cos\frac{\theta}{2}\sin\frac{\theta}{2}d\theta = (R-r)\sin\theta\, d\theta \tag{5}$$

Finally, the values of u_b and v_b are obtained as:

$$u_b = (R-r)\int_0^\theta (1+\cos\theta)d\theta = (R-r)(\theta+\sin\theta) \tag{6}$$

$$v_b = (R-r)\int_0^\theta \sin\theta\, d\theta = (R-r)(1-\cos\theta) \tag{7}$$

And accordingly the velocity and acceleration values of the base mass in horizontal and vertical directions can be written as:

$$\dot{u}_b = 2(R-r)\dot{\theta}\cos^2\frac{\theta}{2} \tag{8}$$

$$\dot{v}_b = (R-r)\dot{\theta}\sin\theta \tag{9}$$

$$\ddot{u}_b = (R-r)\left[2\ddot{\theta}\cos^2\frac{\theta}{2} - \dot{\theta}^2\sin\theta\right] \tag{10}$$

$$\ddot{v}_b = (R-r)\left[\ddot{\theta}\sin\theta + \dot{\theta}^2\cos\theta\right] \tag{11}$$

Based on Equations (6) and (7), the two components of the base mass motion on the rollers can be presented as is shown in Figure 9.

As can be seen in Figure 9, the amount of displacement of the base mass is much more than the roller's displacement. Even in the case of very small amplitude oscillations, in which $\sin\theta \approx \theta$, the

DOI: 10.1002/tal

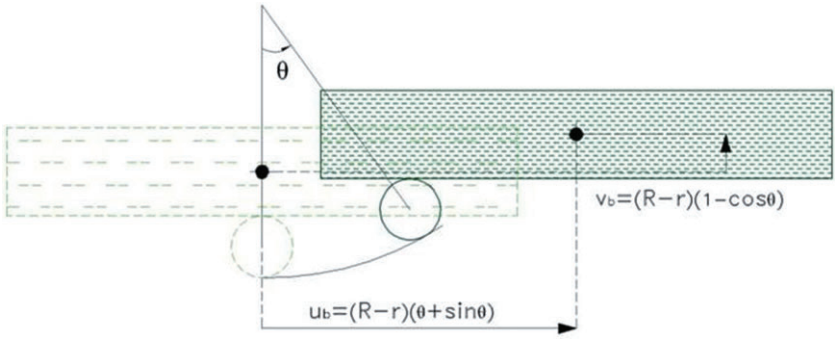

Figure 9. The effect of roller movement on the horizontal and vertical movement of the base mass.

amount of displacement of the base mass is $2(R-r)\theta$, i.e. almost two times of the roller's displacement, $(R-r)\theta$. It should be noted that to derive the equation of motion of the system in various cases, including the basic case, the conventional dynamic equilibrium, which is based on the second Newton law, cannot be used, since the normal reaction forces on the concave beds and the resulting rolling friction forces act at the contact point of the roller with the bed, while all other forces act at the centre of the base mass. In fact, the amount of displacement of the point of action of N_1 and F_{r1} is not the same as the amount of displacement of the point of action of other forces acting on the base mass, and therefore, their effects in creating acceleration in the base mass is not the same. In such cases, the Lagrange equation of motion, which is energy based, is reasonable to be used. Considering θ as the independent generalized coordinate of the system, the Lagrange equation of motion can be written as (Clough and Penzien, 1975):

$$\frac{d}{dt}\left(\frac{\partial T}{\partial \dot{\theta}}\right)-\frac{\partial T}{\partial \theta}+\frac{\partial V}{\partial \theta}=Q \tag{12}$$

where T, V, and Q are respectively kinetic energy, potential energy and the generalized non-conservative force engaged in the system motion, respectively. Based on Figures 7 and 9, which show the basic case, in which $Q = 0$, the energy terms can be written as (inertia and gravity effects of rollers are negligible comparing with those of the system mass):

$$\begin{aligned} T &= \frac{1}{2}m_b(\dot{u}_b^{\,2}+\dot{v}_b^{\,2}) \quad (m_b = \text{the base mass}) \\ &= \frac{1}{2}m_b(R-r)^2\dot{\theta}^2\left(4\cos^4\frac{\theta}{2}+\sin^2\theta\right) \end{aligned} \tag{13}$$

$$V = m_b g(R-r)(1-\cos\theta) \tag{14}$$

Hence:

$$\frac{\partial T}{\partial \dot{\theta}} = m_b(R-r)^2\dot{\theta}(4\cos^4\theta+\sin^2\theta) \tag{15}$$

$$\frac{d}{dt}\left(\frac{\partial T}{\partial \dot{\theta}}\right) = m_b(R-r)^2\left[\ddot{\theta}\left(4\cos^4\frac{\theta}{2}+\sin^2\theta\right)+\dot{\theta}^2\left(\sin 2\theta-8\cos^3\frac{\theta}{2}\sin\frac{\theta}{2}\right)\right] \tag{16}$$

$$\frac{\partial T}{\partial \theta} = m_b(R-r)^2\dot{\theta}^2\left(\sin\theta\cos\theta-4\cos^3\frac{\theta}{2}\sin\frac{\theta}{2}\right) \tag{17}$$

DOI: 10.1002/tal

$$\frac{\partial V}{\partial \theta} = m_b g (R-r)\sin\theta \tag{18}$$

And finally, by substituting the corresponding terms in Equation (12) the Lagrange equation of motion in this case is obtained as:

$$2\ddot{\theta}\cot\frac{\theta}{2} - \dot{\theta}^2 + \frac{g}{R-r} = 0 \tag{19}$$

It is seen that Equation (19) is a nonlinear equation and does not have a classical solution. An appropriate approach for solving this equation is using the fourth order Runge–Kutta numerical method (see Appendix). In the state of small amplitude oscillations or the case in which R has large values, for which the assumption '$\sin\theta \approx \theta$' and neglecting kinetic energy due to vertical velocity and '$\cos\theta \approx 1 - \theta^2/2$' are valid, Equations (6) and (7) change to:

$$u_b \approx 2(R-r)\theta \quad \text{and} \quad v_b \approx (R-r)\frac{\theta^2}{2} \tag{20}$$

$$\dot{u}_b = 2(R-r)\dot{\theta} \tag{21}$$

And therefore, the energy terms and their derivatives can be written as:

$$T \approx \frac{1}{2} m_b \dot{u}_b^{\,2} = 2m_b (R-r)^2 \dot{\theta}^2 \tag{22}$$

$$V \approx m_b g (R-r)\frac{\theta^2}{2} \tag{23}$$

$$\frac{\partial T}{\partial \dot{\theta}} \approx 4m_b (R-r)^2 \dot{\theta} \tag{24}$$

$$\frac{d}{dt}\left(\frac{\partial T}{\partial \dot{\theta}}\right) \approx 4m_b (R-r)^2 \ddot{\theta} \tag{25}$$

$$\frac{\partial T}{\partial \theta} \approx 0 \tag{26}$$

$$\frac{\partial V}{\partial \theta} \approx m_b g (R-r)\theta \tag{27}$$

And finally, the Lagrange equation of motion is written as:

$$\ddot{\theta} + \frac{g}{4(R-r)}\theta = 0 \tag{28}$$

This is a linear equation and its solution is:

$$\theta(t) = A\sin\omega_N t + B\cos\omega_N t \tag{29}$$

where A and B are coefficients related to the initial condition, and:

$$\omega_N = \sqrt{\frac{g}{4(R-r)}} \tag{30}$$

DOI: 10.1002/tal

which gives the natural period of the system in small amplitude oscillations state or the state of large values of R, as:

$$T_N = 4\pi\sqrt{\frac{R-r}{g}} \tag{31}$$

In the case of the prototype sample of the OPRCB isolators whose geometric features are shown in Figure 3, the natural period is calculated as:

$$T_N = 4\pi\sqrt{\frac{0.26-0.01}{9.81}} = 2.006067 \text{ sec}$$

The period value obtained for this case from the response time history, calculated by using fourth order Runge-Kutta method with initial value of 0.15 *rad* for θ, is obtained as 2.006000 sec (see Figure 10), which shows the very high precision of the response calculation method. The high precision of

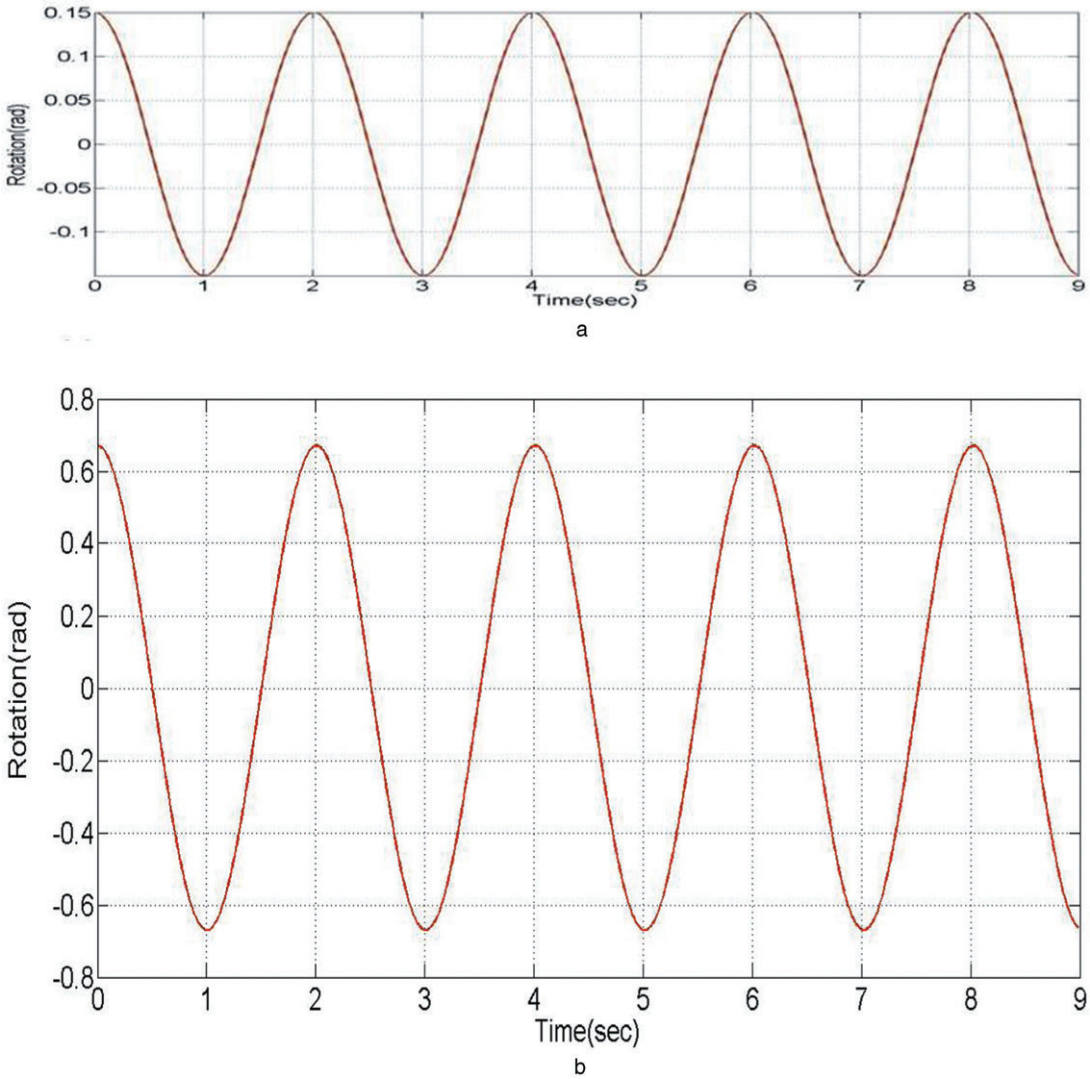

Figure 10. Free vibration response time history of the test sample in absence of rolling friction. (a) for the case of initial value of 0.15 *rad* for θ. (b) for the case of initial value of 0.67 *rad* for θ.

DOI: 10.1002/tal

the response calculation method is confirmed by using other combinations for R and r values as shown in Table 3.

A very interesting finding from response calculations of SDOF system on OPRCB isolator is the independency of the free vibration response frequency/period of the system from the initial values of vibration amplitude, in spite of the nonlinear behaviour of the system due to the concave beds. To show this independency, another sample of response time histories of the prototype sample for the case of initial value of once 0.15 *rad* as a relatively low value, and once 0.67 *rad* for θ, the maximum value for which rotation of rollers can happen without sliding (assuming a value of 0.35 for coefficient of sliding friction), are shown in Figure 10.

It is seen in Figure 10 that the period of free vibration response of the SDOF system on the prototype sample of OPRCB isolator is 2.00 sec regardless of the vibration amplitude. In other words, the natural period of the system is the same for both small and large oscillation states, in the range in which rolling can occur without sliding. It is also worth mentioning that the OPRCB isolators give a hardening stiffness to the isolated SDOF system, which is because of the increase in the bed slope as the lateral displacement of rollers increase. This can be investigated numerically by applying a sinusoidal lateral load having a very long period, which actually creates an almost static condition, to the isolated system and plotting the lateral load—displacement curve of the system, as shown in Figure 11, which has plotted for the prototype sample of OPRCB isolators.

The nonlinear load–displacement behaviour of the OPRCB isolator is seen in Figure 11; however, this nonlinearity does not usually appear since the displacement values are, in most cases, less than 20 cm. To derive the Lagrange equation of motion in the general state with inclusion of all engaged forces, shown in Figure 6, the term of kinetic energy is the same as that given by Equation (13), and

Table 3. Comparison of natural period values of the OPRCB isolator for different values of R and r, in the absence of rolling friction, obtained from Equation (31) and the response time history calculated by Runge–Kutta method

R(m)	r(m)	Classic	Runge–Kutta
0.26	0.01	2.006067	2.006000
0.26	0.02	1.965536	1.966000
0.26	0.03	1.924152	1.924000
0.26	0.04	1.881857	1.882000
0.52	0.01	2.865236	2.866000
0.52	0.02	2.837007	2.837000
1.04	0.01	4.071871	4.072000
1.04	0.02	4.052056	4.052000

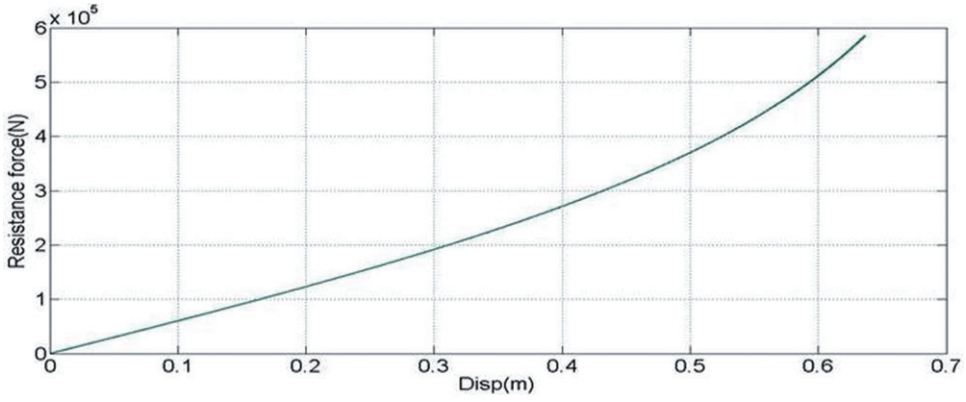

Figure 11. The lateral force–displacement relation of the prototype sample of the OPRCB isolators in static condition, showing its hardening stiffness.

DOI: 10.1002/tal

its corresponding derivatives are the same as those given by Equations (15)–(17), but the term of potential energy is as follows:

$$V = m_b g(R-r)(1-\cos\theta) + \frac{1}{2}k_b(R-r)^2(\theta+\sin\theta)^2 \tag{32}$$

And the term related to the work of non-conservative forces is:

$$\begin{aligned}\delta W_{nc} = &\left[-m_b\ddot{u}_g - c_b 2(R-r)\dot{\theta}\cos^2\frac{\theta}{2}\right](R-r)(1+\cos\theta)\delta\theta \\ &-\text{sign}(\dot{\theta})F_r(R-r)\delta\theta - m_b\ddot{v}_g(R-r)\sin\theta\,\delta\theta\end{aligned} \tag{33}$$

in which F_r is the rolling resistance force given by:

$$F_r = \mu_{r1}N_1 + \mu_{r2}N_2 \tag{34}$$

where N_1 and N_2 with reference to Figure 6 are obtained based on, respectively, vertical equilibrium of rollers and vertical equilibrium of the whole system, as:

$$N_1 = \frac{N_2}{\cos\theta - \text{sign}(\dot{\theta})\mu_{r1}\sin\theta + \tan\frac{\theta}{2}\sin\theta} \tag{35}$$

$$N_2 = m_b(\ddot{v} + \ddot{v}_g + g) \tag{36}$$

In Equations (34) and (35) $\mu_{r(1,2)} = b_1 \cdot \frac{2}{r}$ are the rolling resistance coefficients, where $b_{1,2}$ are parameters given in basic references of physics. Values of rolling resistance coefficient is dependent on the value of normal load between two surfaces and also their curvature, and the values of this coefficient, corresponding to the prototype sample have been obtained by laboratory test in this study, as explained in the next section, and are as given in Table 4.

It is worth mentioning that, as shown in Table 4, the value of rolling resistance is dependent on the value of vertical load. The numbers in the last column of Table 4 are the values of rolling resistant given by the curve fitted to the test results shown in Figure 12.

Based on Equations (15)–(17) and also Equations (32) and (33) the Lagrange equation of motion in the presence of rolling resistance, as well as stiffness and damping forces at the base level, can be written as:

Table 4. Rolling resistance coefficient values obtained from laboratory test on the prototype sample of the OPRDB isolators for different values of vertical load (forces are in N)

N	F_r from laboratory test	μ_r	F_r by the fitted curve
700000	20000	0.0274	19157
600000	13000	0.0244	14661
500000	11000	0.0215	10752
450000	9000	0.0200	9018
400000	8000	0.0186	7430
350000	6500	0.0171	5989
300000	4750	0.0156	4694
250000	3100	0.0142	3546
200000	2500	0.0127	2545
150000	1550	0.0113	1691
100000	1075	0.0098	983

DOI: 10.1002/tal

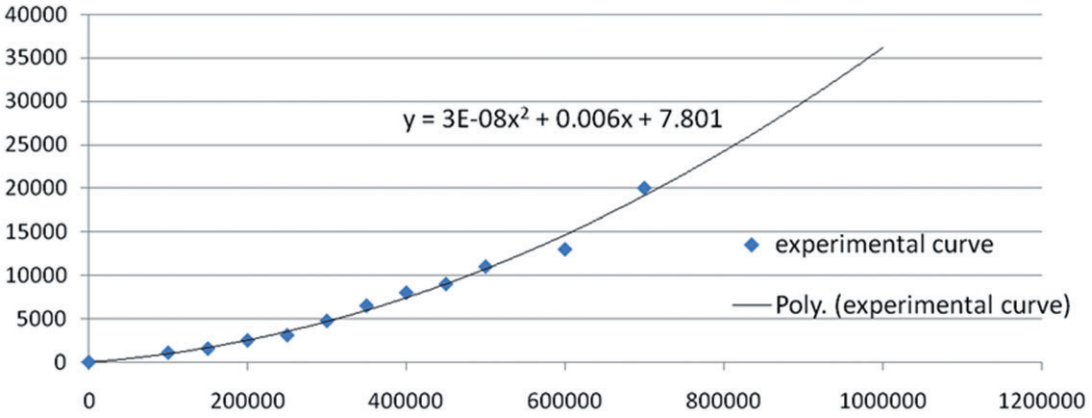

Figure 12. Variation of rolling resistance with vertical load for the prototype sample of OPRCB isolators.

$$2\ddot{\theta}\cot\frac{\theta}{2}-\dot{\theta}^2+\frac{g}{R-r}+\frac{k_b}{m_b}\frac{(1+\cos\theta)(\theta+\sin\theta)}{\sin\theta}=\left[-\frac{\ddot{u}_g}{(R-r)\sin\theta}-\frac{c_b\dot{\theta}\cot\frac{\theta}{2}}{m_b}\right](1+\cos\theta)-\frac{\operatorname{sign}(\dot{\theta})F_r}{m_b(R-r)\sin\theta}-\frac{\ddot{v}_g}{R-r} \tag{37}$$

By solving Equation (37) using the fourth-order Runge–Kutta method, the response time histories of the SDOF system isolated by OPRCB devices can be obtained. To see the effect of rolling friction in the free vibration response of the system, the cases for which the response time histories has been shown in Figure 10 for the frictionless state, have been analysed again, this time, with the inclusion of rolling resistance, of which the results are shown in Figure 13.

Comparing Figure 13 with Figure 10, it can be seen that the rolling friction does not change the natural period of the system, which is 2.00 sec in this case. However, it has an effect very similar to Coulomb damping, leading to linear decrease of free vibration amplitude.

4. EXPERIMENTAL STUDIES OF THE OPRCB ISOLATORS

For studying the performance of the OPRCB isolating devices in different directions and to find out the effect of superstructure's weight on the system performance, some shaking table and cyclic or pseudo-dynamic tests were carried out. At first, by using a shake table of the prototype model, shown in Figure 2(a), the behaviour of the isolating system subjected to lateral excitations were studied. Response histories of the system in two orthogonal directions to the series of harmonic excitations, with frequencies of 0.25, 0.5, 1, 3 and 5 Hz, and also to the El Centro earthquake all applied to the system at an angle of 45° with respect to the main axes of the rollers, were obtained. The masses used in this test were 50 kg, 110 kg and 400 kg but no difference was observed in the value of natural period of the system as expected. Results of these tests can be found in the preliminary report of the study (Kangarloo, 2007).

As the second phase of experimental studies (Kangarloo, 2007), the lower half and the mid plate of the prototype sample were tested by using two actuators, as shown in Figure 14, subjected to various values of vertical loads, starting from 10 tonf, with an increment of 5 tonf, reaching finally a value of 70 tonf, which is around the average gravity load acting on the ground floor columns of a conventional five-storey building.

A sample of the results obtained by pseudo-dynamic tests is shown in Figure 15 for vertical load of 60 tonf and the lateral amplitude of 3.0 cm, which shows the hysteretic behaviour of the OPRCB device.

DOI: 10.1002/tal

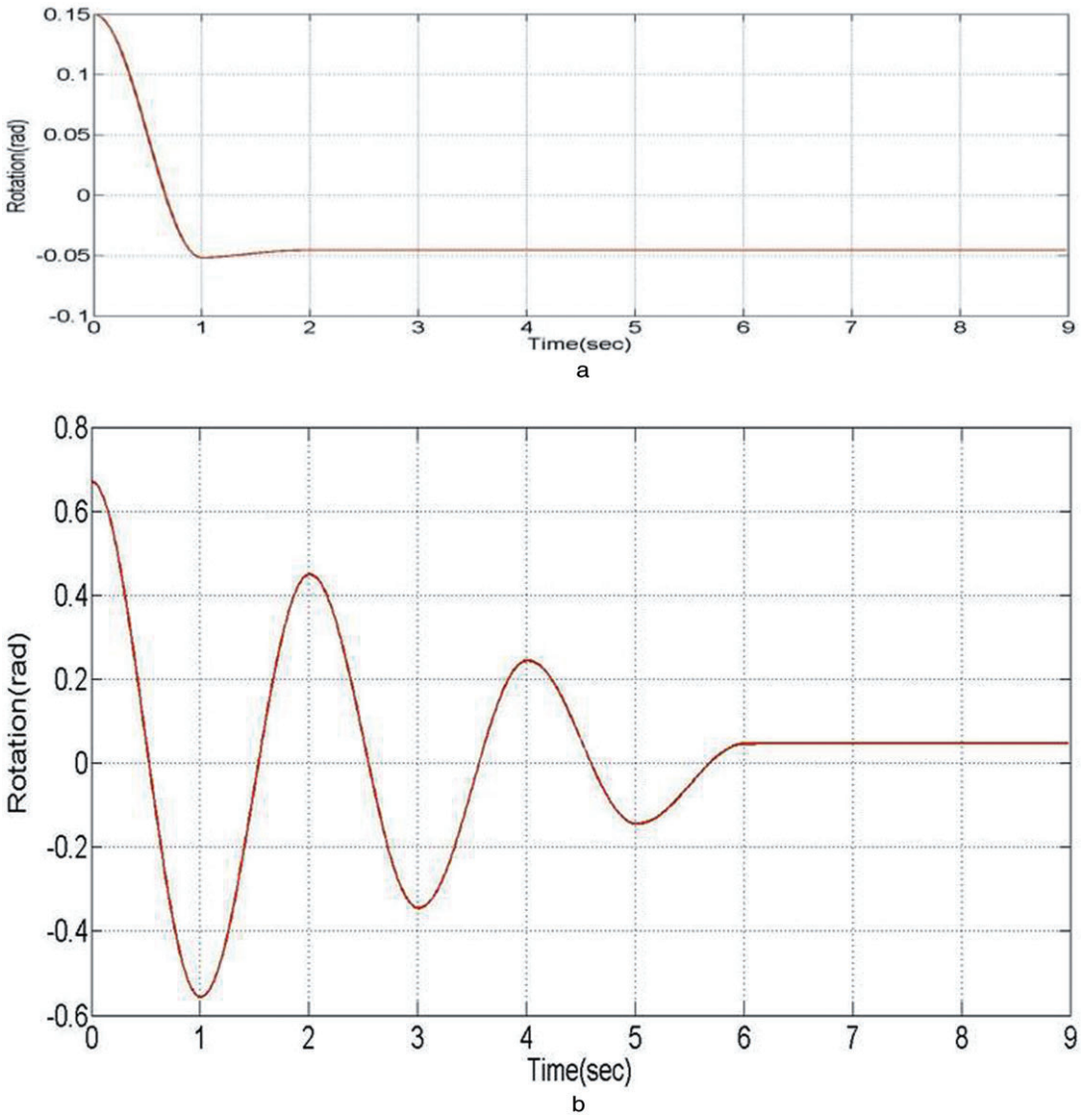

Figure 13. Free vibration response time histories of the prototype sample in presence of rolling friction. (a) for the case of initial value of 0.15 *rad* for θ. (b) for the case of initial value of 0.67 *rad* for θ.

The rolling resistance and the lateral stiffness of the prototype OPRCB isolating system for various vertical loads have been obtained from graphs like the one shown in Figure 15. However, to have these values for the different values of beds and the rollers' radius numerical calculations were necessary, as explained in the next section.

5. NUMERICAL STUDIES OF THE OPRCB ISOLATORS

For numerical studies of the OPRCB isolators, a finite element analysis program was employed and by using very fine meshing, investigating the stress values created in the rollers and their beds at the contact surfaces was tried. A sample of obtained results related to the prototype sample, depicting the values of von Mises stress in rollers and their beds, is shown in Figure 16.

DOI: 10.1002/tal

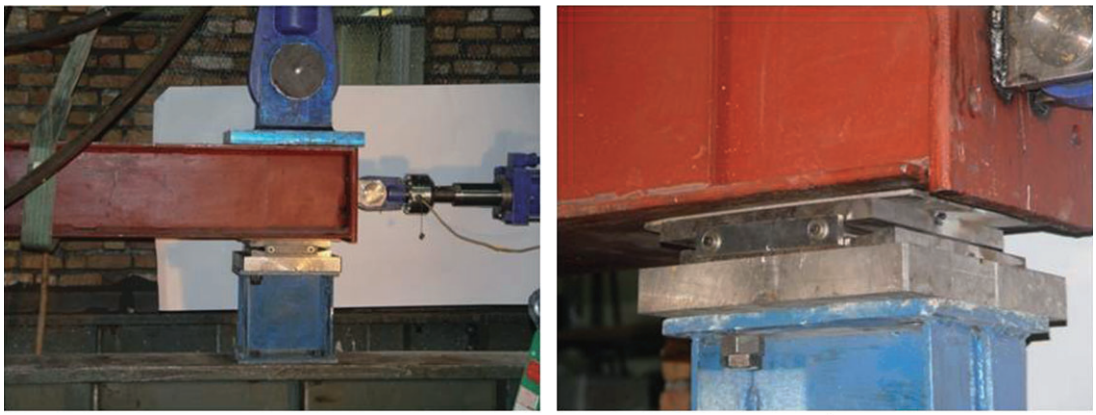

a b

Figure 14. One pair of the OPRCB assembly in pseudo-dynamic test under vertical loads.

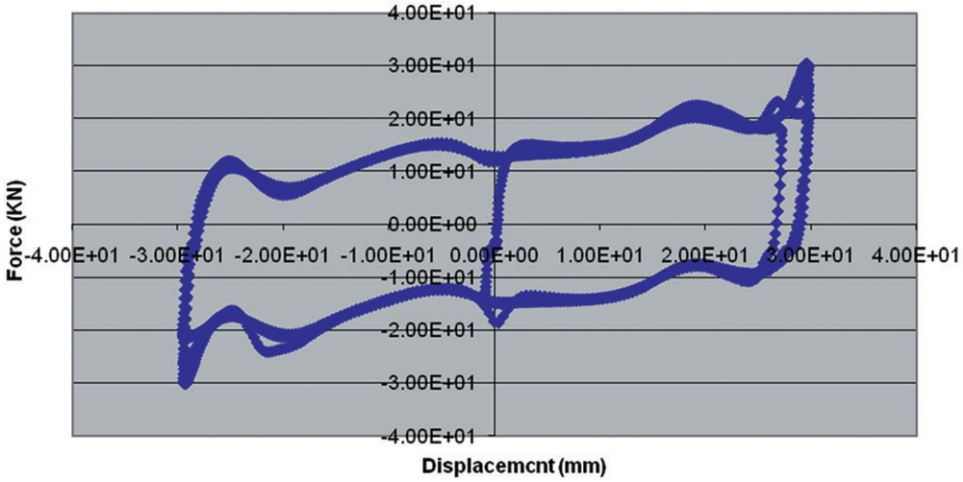

Figure 15. Hysteretic behaviour of the prototype sample under 600 kN vertical load obtained by laboratory test.

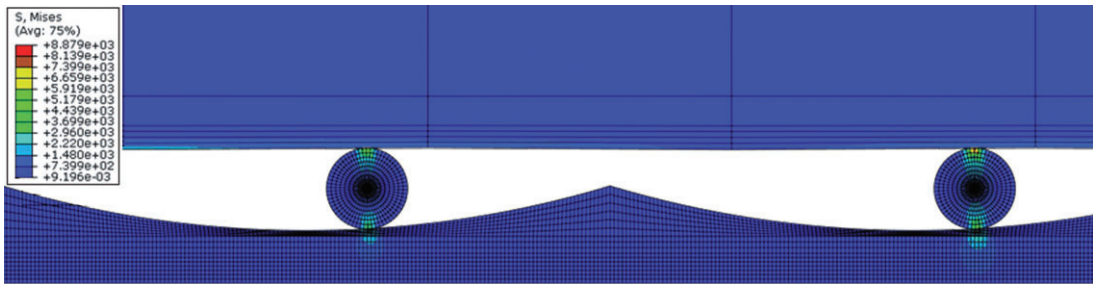

Figure 16. von Mises stresses for the prototype sample shown in Figure 14 in case of 1.0 cm lateral displacement under 600 kN vertical load.

The obtained stress values shows that yielding may not occur in rollers and their bed and the middle plate, provided that they are made of high-strength steel, like MO40 alloy, whose yielding stress is around 900 N/mm^2 (see Table 2). By using the finite element analysis program in large displacement state and employing contact elements between rollers and adjacent surfaces, the hysteretic behaviour

DOI: 10.1002/tal

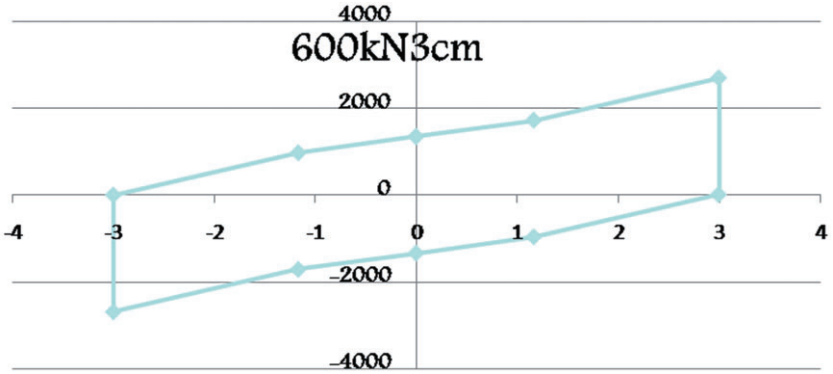

Figure 17. von Mises stresses for the sample shown in Figure 14 in case of 3.0 cm lateral movement under 600 kN vertical load.

of the prototype sample, shown in Figure 14, was obtained for various values of vertical loads (Soroor, 2009). A sample of these numerical results is shown in Figure 17.

Comparison of Figures 15 and 17 (and similar Figures for other cases) shows that the experimental and numerical results are in good agreement, and therefore, it can be said that the values obtained by finite element analyses for rolling resistance and lateral stiffness of OPRCB isolators with different values of beds and rollers' radii are reliable.

6. THE EFFICIENCY OF OPRCB DEVICES IN SEISMIC ISOLATION

To realize the efficiency of the OPRCB devices in seismic isolation of building systems, assuming that the stiffness of the isolated building is high enough to make it reasonable to consider the building as a rigid body with total mass of m_b, equation of motion for the isolated SDOF system, Equation (37) derived in section 3 of the paper, can be used. Omitting the terms of spring and damper forces in this equation changes it to:

$$2\ddot{\theta}\cot\frac{\theta}{2}-\dot{\theta}^2+\frac{g}{R-r}=\left[-\frac{\ddot{u}_g}{(R-r)\sin\theta}\right](1+\cos\theta)-\frac{\operatorname{sign}(\dot{\theta})F_r}{m_b(R-r)\sin\theta}-\frac{\ddot{v}_g}{R-r} \tag{38}$$

Considering that the value of rolling resistance force, F_r, is dependent on the value of rolling resistance coefficient, μ_r, and the values of normal forces between the rollers and their beds (N_1) and middle plate (N_2), and that the values of $\mu_{r(1,2)}$ themselves are dependent on the value of normal forces N_1 and/or N_2, whose values vary during each time step, it seems that the calculations get very complicated. However, since the time step in Runge-Kutta method is very short comparing to the time step of digitized accelerograms, the variation of $N_{1,2}$ during these short time steps can be neglected, and the calculated value of $N_{1,2}$, corresponding to the previous time step, can be used for calculating the value of $\mu_{r(1,2)}$ in the next time step. Furthermore, before calculating the seismic response of the isolated sample building, its response to a very low frequency (very long period) sinusoidal load was calculated based on Equation (38) to see if the static behaviour of the system can be obtained from its dynamic behaviour when the loading speed is very low. Figure 18 shows such a hysteretic response of the isolated system under 600 kN vertical load.

Comparison of Figure 18 with Figures 15 and 17 shows that experimental results, finite element analysis results and numerical results of dynamic model are all in good agreement. From these figures, the energy dissipation capacity of the proposed isolation device can be also realized. This energy dissipation capacity depends directly on the rolling resistance coefficient of the system, $\mu_{1,2}$, and contrarily on the radius of the concave beds, R. This energy dissipation capability of the system due to its rolling resistance gives the system a damping property which leads to linear decrease of its free vibration amplitude, as shown in Figure 13 in section 3 of the paper.

DOI: 10.1002/tal

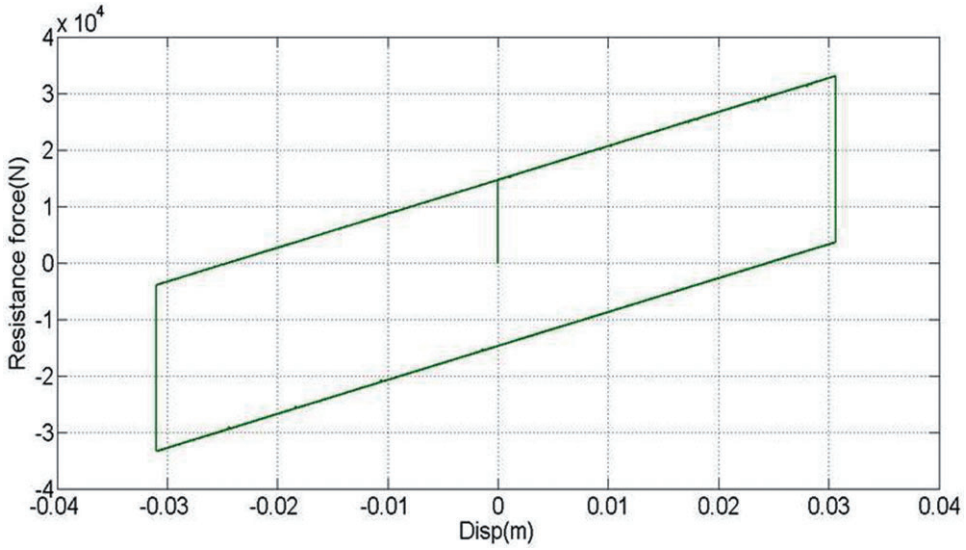

Figure 18. Hysteretic loop of the prototype sample under 600 kN vertical load obtained by very low frequency dynamic Analysis.

To show the efficiency of the OPRCB isolating system in decreasing the earthquake effect on the isolated systems, the seismic responses of an SDOF system with a mass of 70 ton (almost equivalent to the mass corresponding to each column of a five-storey building) and natural period of 0.5 sec in fixed-base state, once with fixed base and once isolated have been calculated to the simultaneous effect of the horizontal and vertical components of Tabas, Iran earthquake of 1978 with its Peak Ground Acceleration (PGA) normalized to 0.5 g. The time histories and spectra of Tabas earthquake and the calculated responses are shown in Figures 19–23.

It can be seen in Figures 20–23 that the peak displacement response of isolated system is almost twice as its fixed-base response, while its peak absolute acceleration response is just around 12% of its fixed-base response. It is also noticeable that the peak displacement response of the isolated system is almost 1/3rd of the maximum ground displacement and its peak acceleration response is almost 1/4th of the PGA value of the record. Response histories obtained for other values of bed's and rollers' radii show that the responses can be controlled easily for each earthquake and getting lower absolute acceleration responses is possible (Soroor, 2009).

The other point that is worth investigating with regard to the OPRCB isolators is their energy absorption capacity due to rolling resistance. For this purpose, the graphs showing the hysteretic behaviour of isolators is a very useful means. A sample of these graphs is shown in Figure 24.

It is seen in Figure 24 that the system has had an effective stiffness of around 670 000 N/m, which, considering its mass of 70 tons, gives an effective natural frequency of 9.57 rad/sec or effective natural period of 2.03 sec, which is quite close to the corresponding value of 2.00 sec, given by analytical formula. This figure also shows that the system has dissipated a relatively large amount of energy, and this can be the reason behind its relatively low peak displacement response (almost 1/3 of the peak ground displacement), in spite of its relatively long period.

7. CONCLUSIONS

Based on the analytical formulations, the experimental and numerical results, and also the dynamic response calculations of the SDOF systems isolated by OPRCB devices, it can be concluded that:

(1) The OPRCB seismic isolating system has a good performance for low- to mid-rise buildings and can reduce the earthquake induced forces drastically by reducing the total acceleration of the isolated system up to ten times comparing to the fixed-base system.

DOI: 10.1002/tal

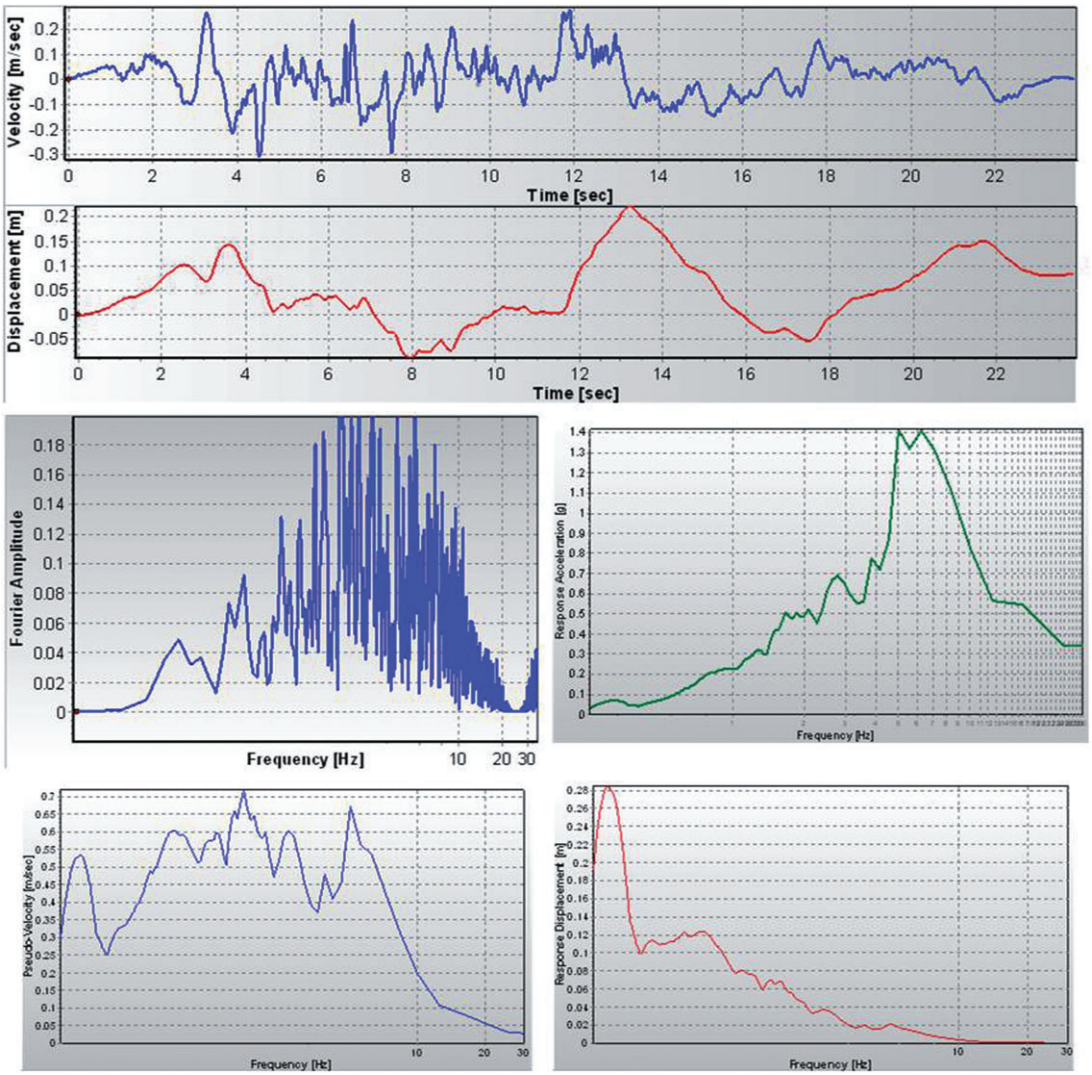

Figure 19. Tabas earthquake records and Fourier and response spectra.

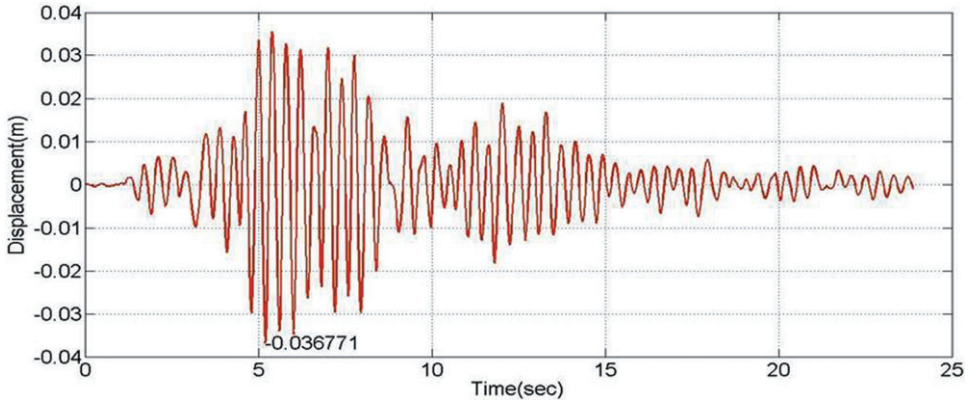

Figure 20. Displacement response history of the fixed-base equivalent five-storey building subjected to Tabas Earthquake.

DOI: 10.1002/tal

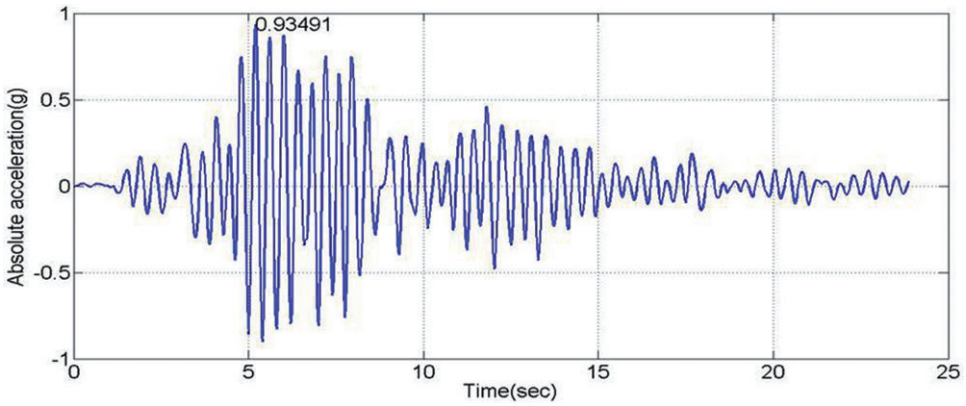

Figure 21. Acceleration response history of the fixed-base equivalent five-storey building subjected to Tabas Earthquake.

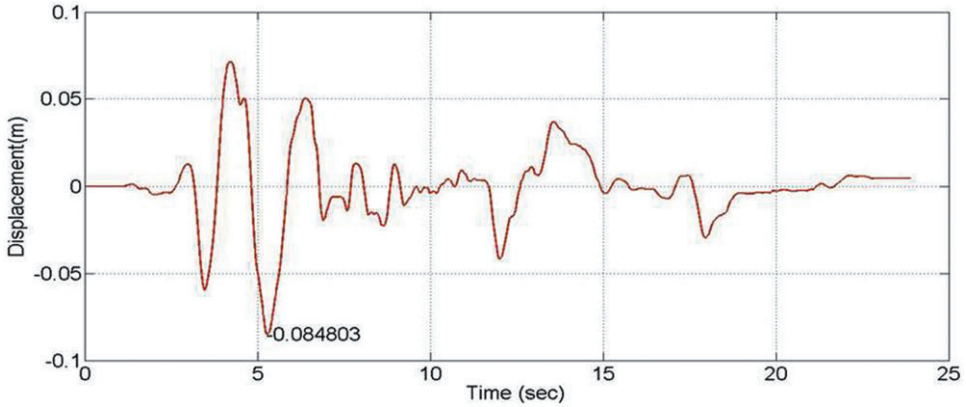

Figure 22. Displacement response history of the equivalent five-storey building isolated by the prototype OPRCB device subjected to Tabas Earthquake.

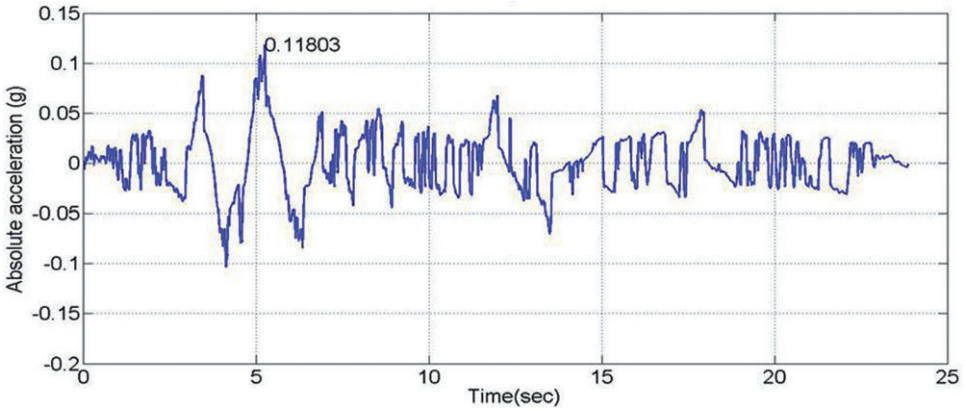

Figure 23. Acceleration response history of the equivalent 5-storey building isolated by the prototype OPRCB device subjected to Tabas Earthquake.

DOI: 10.1002/tal

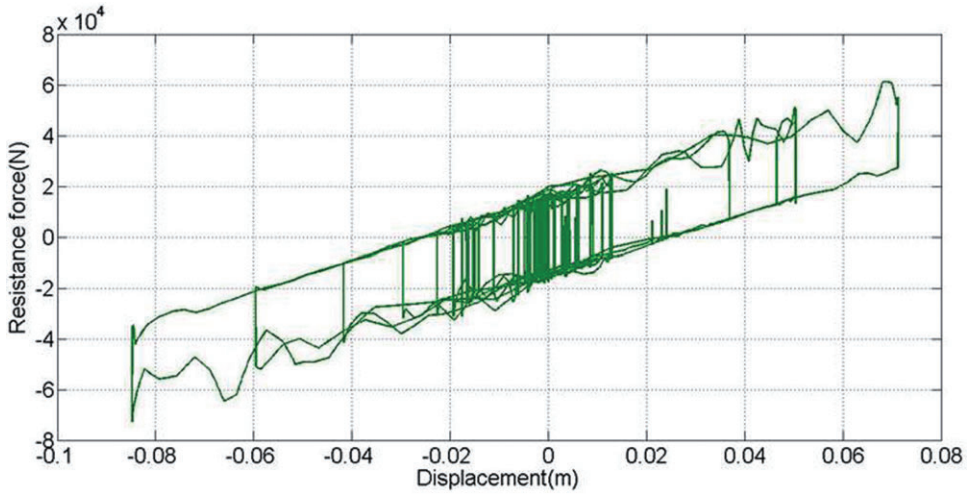

Figure 24. Resistance force on an earthquake.

(2) The effective natural period of the isolated system can be easily controlled by the ratio of rollers' radius to concave bed's radius (*r/R*), and achieving a period of 2.5 seconds or more is possible with no difficulty.
(3) The proposed isolating device can have an energy dissipating capability whose amount depends on the rolling resistance coefficient between rollers and adjacent surfaces, which is itself a function of the hardness of surfaces, the radii of rollers and their concave bed, and the building weight.
(4) In spite of the nonlinear force–displacement behaviour of the OPRCB isolators, the natural period of the SDOF system isolated by this device is basically constant (independent of the displacement amplitude), for a given value of *r/R*, and the rolling resistance gives a damping of the Coulomb type to the system.
(5) The maximum lateral displacement of the system under earthquake excitations can be kept limited to a few centimetres by using lower values of *R*. However, using low *R* values in some cases may cause the maximum acceleration transferred to the isolated system not to be reduced to the desired level.
(6) The advantages of OPRCB isolators, including simplicity of production and installation, low cost, and relatively small dimensions and low weight, are very encouraging for proposing its practical use in low- to mid-rise buildings.

Finally, it should be noted that keeping the dimensions of the OPRCB base isolators as low as possible is very important for practical advantages. However, in case of some near-field earthquakes, in which occurrence of a large amplitude long period pulse is likely, the maximum displacement which the isolator should facilitate may be very large. To assure how large this displacement may need to be, more investigations are required.

REFERENCES

Buckle IG, Mayes RL. May 1990. Seismic isolation: history, application, and performance—a world view. *Earthquake Spectra* **6**(2): 161–201.

Chung LL, Yang CY, Chen HM, Lu LY. 2009. Dynamic behavior of nonlinear rolling isolation system. *Structural Control and Health Monitoring* **16**(1): 32–54. Special Issue: Part 1: Selected Papers from International Symposium on Structural Control and Health Monitoring, Taichung, Taiwan, January 10–11, 2008.

Hanai T, Nakata S, Kiriyama S, Fukuwa N. 2004. Comparison of seismic performance of base-isolated house with various devices. In *Proceedings of the 13th World Conference on Earthquake Engineering*, Vancouver, Canada, 01–06 August, Paper No. 1203.

Hart GC, Wong, K. 2000. *Structural Dynamics for Structural Engineers*. John Wiley & Sons, Inc.: New York.

DOI: 10.1002/tal

Hosseini M, Kangarloo K. 2007. Introducing orthogonal rollers pairs as an effective isolating system for low rise buildings. In *Proceedings of the 6th International Conference on Earthquake Resistant Engineering Structures (ERES 2007)*, 11–13 June, Bologna, Italy, 151–161.

Hosseini M, Soroor A. 2009. A study on the use of orthogonal pairs of rods on concave beds (OPRCB) as a base isolation device for building systems. In *Proceedings of the 8th International Congress on Civil Engineering*, Shiraz University, Shiraz, Iran, 11–13 May; Paper S5000.

Jangid RS. 1995. Seismic response of structures isolated by free rolling rods. *European Earthquake Engineering* **3**:3–11.

Jangid RS. 2000. Stochastic seismic response of structures isolated by rolling rods. *Engineering Structures* **22**: 937–946.

Jangid RS, Datta TK. 1995. Seismic behavior of base isolated building–a state-of-the-art review. *Journal of Structures and Buildings* **110**: 186–203.

Jangid RS, Londhe YB. 1998. Effectiveness of elliptical rolling rods for base isolation. *Journal of Structural Engineering, ASCE* **124**: 469–72.

Kangarloo, K. 2007. Experimental studies on orthogonal rollers pairs as an isolating system for low- to mid-rise buildings. MS Thesis, Islamic Azad University (IAU).

Lee GC, Liang ZA. 2003. Sloping surface roller bearing and its lateral stiffness measurement. In *Proceedings of the 19th US–Japan Bridge Engineering Workshop*, Tsukuba, Japan, 27–30 October, 27–29.

Lee GC, Liang Z, Niu TC. 2003. Seismic Isolation Bearing. US Patent application publication, Pub. No. US2003/0099413 A1, 29 May.

Lee GC, Ou Y-C, Song J, Niu T, Liang, Z. 2008. A roller seismic isolation bearing for highway bridges. In *Proceedings of the 14th World Conference on Earthquake Engineering: Innovation Practice Safety*, Beijing, China, 12–17 October, Paper ID 11-0140.

Lin TW, Hone C. 1993. Base isolation by free rolling rods under basement. *Earthquake Engineering and Structural Dynamics* **22**: 261–273.

Lin TW, Chern CC, Hone CC. 1995. Experimental study of base isolation by free rolling rods. *Earthquake Engineering and Structural Dynamics* **24**: 1645–1650.

Londhe YB, Jangid RS. 1999. Dynamic response of structures supported on elliptical rolling rods. *Journal of Structural Mechanics and Earthquake Engineering, JSCE* **16**(1): 1s–10s.

Naeim F, Kelly JM. 1999. *Design of Seismic Isolated Structures: From Theory to Practice*. John Wiley & Sons Inc: New York.

Soroor A. 2009. Analytical study of effectiveness of orthogonal rolling rods isolation system in mid-rise Regular buildings. MS Thesis, Islamic Azad University (IAU).

Tsai M-H, Chang K-C, Wu S-Y. 2006. Seismic Isolation of a Scaled Bridge Model Using Rolling-Type Bearings, In *Proceedings of the 4th International Conference on Earthquake Engineering*, Taipei, Taiwan, 12–13 October 2006, Paper No. 181.

Tsai M-H, Wu S-Y, Chang K-C, Lee GC. 2007. Shaking table tests of a scaled bridge model with rolling-type seismic isolation bearings. *Engineering Structures* (29): 694–702.

Wegst CW, Stahlchlüssel/Key to steel/la clé des aciers, 2007. CD-ROM 1–3 users floating license, Langue: Français & Anglais & Allemand, Etat: Disponible Chez L'éditeur.

Zhou FL. 2001. Seismic isolation of civil buildings in the People's Republic of China. *Progress in Structural Engineering and Materials* **3**: 268–276.

Zhou FL, Stiemer SF, Cherry S. 1988. Design method of isolating and energy dissipating system for earthquake resistant structures. In *Proceedings of the 9th World Conference on Earthquake Engineering*, Tokyo-Kyoto, Japan, August; **3**: 397–402.

APPENDIX: THE MODIFIED 4TH ORDER RUNGE-KUTTA METHOD

Eq. (19) in section 2 of the paper, $\left[2\ddot{\theta}\cot\frac{\theta}{2}-\dot{\theta}^2+\frac{g}{R-r}=0\right]$ is a second order differential equation which does not have any analytical solution. The modified 4th order Runge-Kutta method is used for such equations, in which just the first and the second derivatives appear in the differential equation with the main unknown function. This method has more precision and is less time-consuming, and its trend is as follows. Considering the time as the main variable of the problem, and writing the second order differential equation for the n^{th} time instant as:

$$\ddot{Y} = f\left(t_n, Y_n, \dot{Y}_n\right)$$

The four algebraic terms K_1 to K_4 are calculated as follows,

$$K_1 = \frac{h^2}{2} f\left(t_n, Y_n, \dot{Y}_n\right)$$

DOI: 10.1002/tal

$$K_2 = \frac{h^2}{2} f\left(t_n + \frac{h}{2}, Y_n + \frac{h\dot{Y}_n}{2} + \frac{K_1}{4}, \dot{Y}_n + \frac{K_1}{h} \right)$$

$$K_3 = \frac{h^2}{2} f\left(t_n + \frac{h}{2}, Y_n + \frac{h\dot{Y}_n}{2} + \frac{K_1}{4}, \dot{Y}_n + \frac{K_2}{h} \right)$$

$$K_4 = \frac{h^2}{2} f\left(t_n + h, Y_n + h\dot{Y}_n + K_3, \dot{Y}_n + \frac{2K_3}{h} \right)$$

where h is the size of the time step (to which an appropriate value should be assigned to result in a desired precision level of the solution) and t_n is the value of the n^{th} time instant. Now, the values of the unknown function and its first derivative in the n + 1 time instant can be calculated as:

$$Y_{n+1} = Y_n + h\dot{Y}_n + \frac{K_1 + K_2 + K_3}{3}$$

$$\dot{Y}_{n+1} = \dot{Y}_n + \frac{K_1 + 2K_2 + 2K_3 + K_4}{3\,h}$$

DOI: 10.1002/tal